Circulation

ORIGINAL RESEARCH ARTICLE

Human Engineered Heart Tissue Patches Remuscularize the Injured Heart in a Dose-Dependent Manner

BACKGROUND: Human engineered heart tissue (EHT) transplantation represents a potential regenerative strategy for patients with heart failure and has been successful in preclinical models. Clinical application requires upscaling, adaptation to good manufacturing practices, and determination of the effective dose.

METHODS: Cardiomyocytes were differentiated from 3 different human induced pluripotent stem cell lines including one reprogrammed under good manufacturing practice conditions. Protocols for human induced pluripotent stem cell expansion, cardiomyocyte differentiation, and EHT generation were adapted to substances available in good manufacturing practice quality. EHT geometry was modified to generate patches suitable for transplantation in a small-animal model and perspectively humans. Repair efficacy was evaluated at 3 doses in a cryo-injury guinea pig model. Human-scale patches were epicardially transplanted onto healthy hearts in pigs to assess technical feasibility.

RESULTS: We created mesh-structured tissue patches for transplantation in guinea pigs (1.5×2.5 cm, 9–15×10^6 cardiomyocytes) and pigs (5×7 cm, 450×10^6 cardiomyocytes). EHT patches coherently beat in culture and developed high force (mean 4.6 mN). Cardiomyocytes matured, aligned along the force lines, and demonstrated advanced sarcomeric structure and action potential characteristics closely resembling human ventricular tissue. EHT patches containing ≈4.5, 8.5, 12×10^6, or no cells were transplanted 7 days after cryo-injury (n=18–19 per group). EHT transplantation resulted in a dose-dependent remuscularization (graft size: 0%–12% of the scar). Only high-dose patches improved left ventricular function (+8% absolute, +24% relative increase). The grafts showed time-dependent cardiomyocyte proliferation. Although standard EHT patches did not withstand transplantation in pigs, the human-scale patch enabled successful patch transplantation.

CONCLUSIONS: EHT patch transplantation resulted in a partial remuscularization of the injured heart and improved left ventricular function in a dose-dependent manner in a guinea pig injury model. Human-scale patches were successfully transplanted in pigs in a proof-of-principle study.

Eva Querdel*
Marina Reinsch, PhD*
Liesa Castro, MD*
⋮
Thomas Eschenhagen, MD†
Florian Weinberger, MD†

The full author list is available on page 2004.

*E. Querdel, M. Reinsch, and L. Castro contributed equally.

†T. Eschenhagen and F. Weinberger contributed equally.

Key Words: cell transplantation ■ regenerative medicine ■ stem cells

Sources of Funding, see page 2005

https://www.ahajournals.org/journal/circ

ORIGINAL RESEARCH ARTICLE

Clinical Perspective

What Is New?

- Human engineered heart tissue patches can be generated under good manufacturing practice–compatible conditions and in human scale (5×7 cm, 450×10^6 cells).
- Engineered heart tissue patch transplantation remuscularizes the injured heart in a dose-dependent manner.
- Cardiomyocyte proliferation after transplantation participates in graft development.

What Are the Clinical Implications?

- Engineered heart tissue transplantation might provide a new therapeutic strategy for patients with heart failure.
- Stimulation of cardiomyocyte proliferation after transplantation could represent a strategy to improve transplantation success.

Heart disease is the number one cause of death worldwide.[1] Although mortality from acute myocardial infarction has decreased substantially over the past 2 decades,[2] heart failure as its main sequela remains a major disease burden.[3] Cardiomyocyte renewal is limited to ≈1% per year, and, even though there is evidence that cardiomyocyte proliferation increases slightly after injury, this is by far too little to form a physiologically relevant number of new cardiomyocytes.[4]

Regenerative strategies that aim to generate new myocardium are currently being evaluated in preclinical[5] and first clinical trials.[6,7] Pluripotent stem cell–derived cardiomyocytes have repeatedly demonstrated their potential to regenerate injured hearts in preclinical models.[8–11] We have recently shown that transplantation of 2 strip-format human engineered heart tissues (EHTs) improved left ventricular function in a guinea pig model.[9] Yet, hurdles toward clinical translation remain. Upscaling from small-animal models to humans and adaptation to good manufacturing practices (GMPs) represent challenges. In addition, the optimal dose has not yet been defined. The present study describes the generation of EHT patches under GMP-compatible conditions that can be scaled to a clinically relevant size, evaluated the effect of EHT-patch transplantation in a dose-finding study in guinea pigs, and assessed the possibility to transplant human-scale EHT patches in pigs.

METHODS

All data associated with this study are present in the article or the Data Supplement. Materials will be available from the corresponding author by request.

Animal Care and Experimental Protocol Approval

The investigation conforms to the guide for the care and use of laboratory animals published by the National Institutes of Health (Publication No. 85-23, revised 1985) and was approved by the local authorities (Behörde für Gesundheit und Verbraucherschutz, Freie und Hansestadt Hamburg: 85/12, 97/14 61/15 and 109/16 and Regierung von Oberbayern: 02-18-134).

Human Induced Pluripotent Stem Cell Culture and Cardiac Differentiation

UKEi1-A was reprogrammed with a Sendai Virus strategy (CytoTune iPS Sendai Reprogramming Kit, ThermoFisher). These studies were approved by the Ethical Committee of the University Medical Center Hamburg-Eppendorf (Az. PV4798/28.10.2014 and Az. 532/116/9.7.1991). C25 was kindly provided by A. Moretti.[12] The human induced pluripotent stem cell (hiPSC) line TC-1133 was obtained from the National Institute of Neurological Disorders and Stroke Human Cell and Data Repository (Rutgers University).[13] The expansion and cardiac differentiation of hiPSC were performed as recently described.[14] Antibodies used for characterization are listed in Table I in the Data Supplement.

EHT Generation

EHTs were generated from cells and fibrinogen/thrombin as previously described.[9] For this study, the devices for casting and culturing EHTs were adapted to reach the geometries required for the intended use. Standard EHT patches (1.5×2.5 cm) were generated in a 6-well format (Figure I in the Data Supplement) with 9 to 15×10^6 hiPSC cardiomyocytes per 1.5 mL. For human-scale EHT patches (5.0×7.0 cm) 430 to 450×10^6 cells were resuspended in 25 mL.

GMP-Compliant Culture Conditions

Culture conditions for hiPSC expansion, cardiac differentiation, and EHT cultivation were adapted to contain only reagents that are available at GMP grade. For economic reasons, non-GMP versions of these reagents were used during this study. Changes from the above-stated standard protocol were as follows: (1) The hiPSC culture substrate was changed to human vitronectin (Gibco No. A27940, at 0.5 µg/cm^2). (2) To apply a defined B27 serum-replacement reagent, all B27 components were mixed according to the Hanna Laboratory protocol (Weizmann Institute of Science), apart from superoxide dismutase, which was omitted in our protocol. (3) Matrigel was omitted during EHT generation. (4) Horse serum was replaced by human serum (see Table II in the Data Supplement).

Action Potential Recordings

Sharp microelectrodes were used to record action potentials (APs) as described previously[15,16] in intact EHTs or left ventricular tissue superfused with Tyrode solution containing (in mmol/L): NaCl 127, KCl 5.4, $MgCl_2$ 1.05, $CaCl_2$ 1.8, glucose 10, $NaHCO_3$ 22, $NaHPO_4$ 0.42, equilibrated with O_2-CO_2 (95:5) pH 7.4 at 36.5±0.5 °C. Field stimulation was used to

Circulation. 2021;143:1991–2006. DOI: 10.1161/CIRCULATIONAHA.120.047904

pace the tissues. Multiple APs (>5) were measured in each tissue preparation and the n numbers given are the numbers of EHTs or left ventricular samples.

Conduction Velocity Measurement

Conduction velocity was calculated by measuring the delay from a stimulation artifact to the upstroke of an AP at different locations.

Contractility Studies

The EHT patch was mounted in a 50-mL organ bath, with 1 end of the construct clamped down between a pair of platinum electrodes and the free end tied to a strain gauge. Force was measured under spontaneous beating. Resting tension was adjusted to yield approximately half-maximum active force development.

Injury Model and EHT Patch Transplantation

Myocardial injury was induced as previously described.[9] Cryo-injury of the left ventricular wall was induced in female guinea pigs (300–450 g, 8–9 weeks of age, Charles River and Envigo). Patch EHTs were sutured above the scar 7 days after injury. Care was taken to suture the patch onto the healthy myocardium adjacent to the scar. To vary the dosage of the applied cardiomyocyte number, we generated EHTs with different cell densities (cell-free, fibrin patches without cells; dose 1, 9×10^6 cells; dose 2, 12×10^6 cells; and dose 3, 15×10^6 cells per 1.5 mL). Because cell number influences EHT development,[17] it was not possible to only decrease cardiomyocyte number per patch. We therefore used a strategy combining cell number and patch area to create patches with different cell content. Increasing portions of EHTs from dose 1, 2, and 3 were transplanted to reach the desired total cell numbers: dose 1, 50% ($\approx4.5\times10^6$ cells); dose 2, 70% ($\approx8.5\times10^6$ cells); and dose 3, 80% (12×10^6 cells) that were all sufficient in size to cover the whole injury site. Surgeons were blinded regarding the EHT patch cell content (except for cell-free constructs). Guinea pigs were immunosuppressed with cyclosporine beginning 3 days before transplantation (7.5 mg/kg body weight per day for the first 3 postoperative days and 5 mg/body weight per day for the following 25 days; mean plasma concentration, 608 µg/L) and methylprednisolone (2 mg/kg body weight per day).

Echocardiography

Echocardiography was performed with a Vevo 3100 System (Fujifilm VisualSonics) as previously described.[9] Echocardiography was performed in all animals in the dose-finding study (n=75). Because of technical problems with the echocardiography system, a few animals that were already included in the study did not receive all 3 echocardiographies (baseline, n=4; postinjury, n=4; 4 weeks posttransplantation, n=2). Analysis was performed in a blinded manner.

Organ Preparation and Histology

Hearts were processed for histology as recently described.[9] The antibodies used are summarized in Table III in the Data Supplement.

EHT Patch Transplantation in Pigs

Transgenic pigs overexpressing LEA29Y, a human CTLA4-Ig derivate, were generated as described previously.[18] Pigs (LEA29Y: n=4; wildtype: n=5) were anesthetized as previously described[19] and underwent left-sided lateral thoracotomy. The heart was exposed, and the pericardium was opened. EHT patches (n=6 patches/N=5 animals) or human-scale patches (n=3 patches/N=4 animals; 1 patch was divided in 2 parts immediately before transplantation) were sutured onto the healthy myocardium. Afterward, pigs were pharmacologically immunosuppressed with methylprednisolone (250 mg on the day of surgery and 125 mg/d starting at day 1 after surgery), tacrolimus (0.2 mg/kg body weight per day), and mycophenolate mofetil (40 mg/kg body weight per day). Wildtype animals additionally received belatacept (10 mg/kg body weight per day on the day of surgery and 4 days after surgery). Animals were regularly monitored and euthanized under deep anesthesia by intravenous injection of saturated KCl (1–2 weeks after transplantation).

Statistics

Statistical analyses were performed with GraphPad Prism 6 or GraphPad Prism 9. Comparison among 2 groups was made by 2-tailed unpaired Student *t* test. One-way ANOVA followed by the Tukey test for multiple comparisons was used for >2 groups. When 2 factors affected the result (eg, time point and group), 2-way ANOVA analyses and the Tukey test for multiple comparisons were performed. Error bars indicate SEM. *P* values are displayed graphically as follows: * $P<0.05$, ** $P<0.01$, *** $P<0.001$.

RESULTS

Generation of Human EHT Patches

Standard mini EHTs (≈8×1 mm) for drug screening and disease modeling are generated in a 24-well format.[20] We have previously simply upscaled the strip size for transplantation.[9] For this study, we aimed to further improve the EHT geometry for transplantation and create patches that (1) resemble human myocardium, (2) cover the scar in a small-animal model, and (3) allow for further scaling to a human size (Figure I in the Data Supplement). Initial attempts without mesh structure resulted in patches in which cardiomyocyte density was sparse (Figure I in the Data Supplement). We then generated medium-sized EHT patches ($9–15\times10^6$ cells) with a mesh structure by adopting previously described protocols[9,21] (Figure 1A). Cardiomyocytes for these patches were differentiated from 3 different iPSC-cell lines (C25; UKEi1-A; TC-1133, troponin-T positivity 83±1.5%; n=24).

Over a 3-week culture period, EHT patches remodeled and decreased in width (Figure 1A). Single beating cardiomyocytes were visible within 24 hours after casting. Histology showed immature cardiomyocytes at day 1 (Figure 1B). Macroscopically visible contractions started between day 10 and 15 after casting. Initial beating was

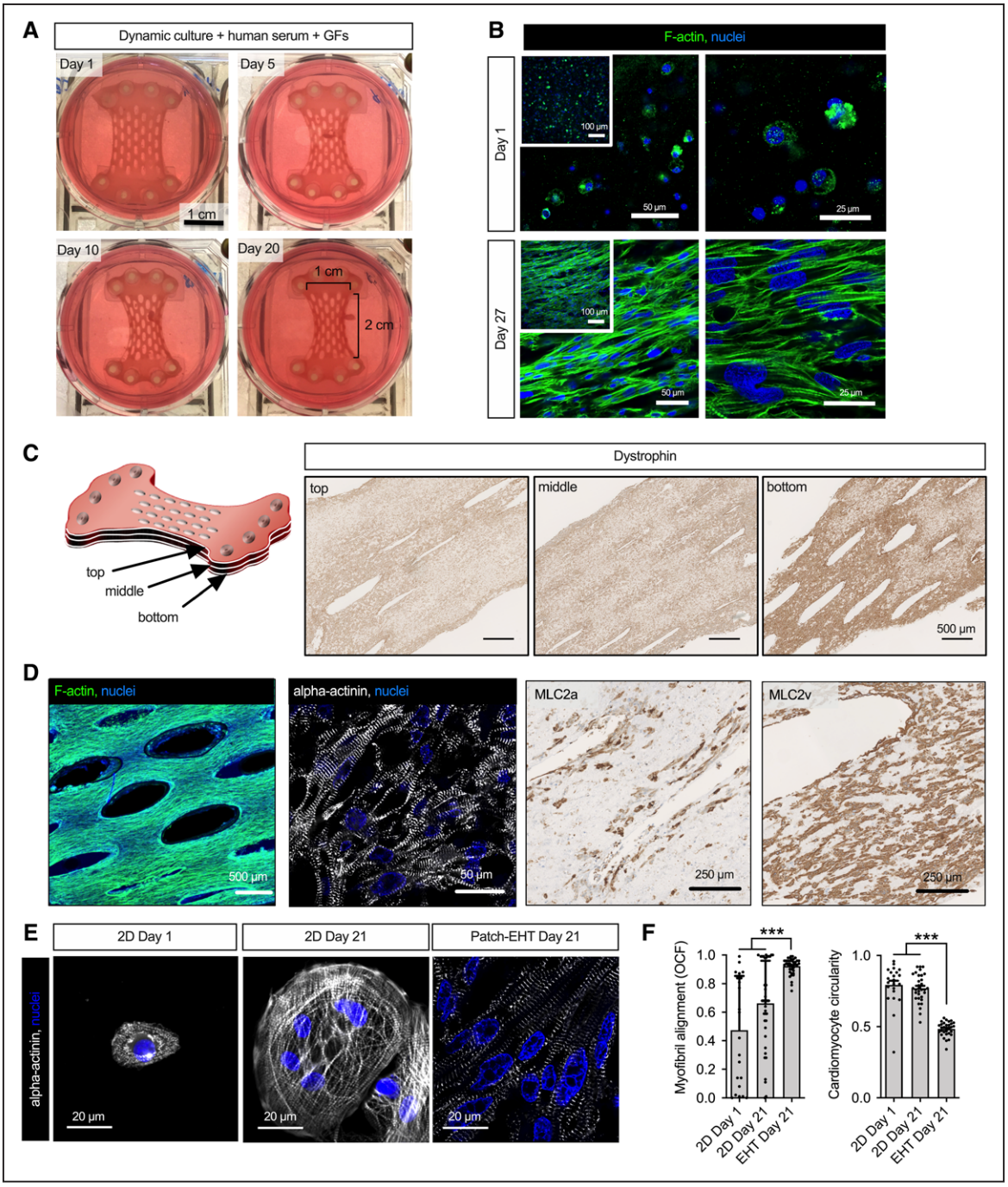

Figure 1. Characterization of human engineered heart tissue patches.
A, Photographs of EHT patches demonstrating EHT development over a 3-week culture period. **B**, Phalloidin staining of human EHT patches at day 1 and day 27 after casting. Insets show low magnification overviews. **C**, Serial longitudinal sections stained for dystrophin. Shown are sections from the upper and lower surface and the middle of the EHT patch, respectively. **D**, Phalloidin whole mount and α-actinin, myosin light chain, atrial isoform, and myosin light chain, ventricular isoform staining in longitudinal sections after 21 days in culture. Analysis (**E**) and quantification (**F**) of sarcomeric organization and circularity of human induced pluripotent stem cell–derived cardiomyocytes in EHT patches compared with 2-dimensional (2D) culture. Myofibril alignment expressed as orientation correlation function (OCF). A value of 1 either indicates parallel alignment (OCF) or a perfect circle (circularity; n=10–15 cells/N=3 EHT patches or cell culture preparations; each data point represents 1 cell). Statistical analyses were performed by 1-way ANOVA followed by the Tukey test for multiple comparisons. Mean±SEM values are shown, ***P<0.001. EHT indicates engineered heart tissue; and GFs, growth factors.

asynchronous, indicating competing pacemaker centers, but converted to a coherent, synchronous beating pattern after an additional 3 to 5 days in culture (Movies I and II in the Data Supplement) that was mirrored by structural signs of tissue maturation (Figure 1B).

Within 3 weeks, cardiomyocytes aligned along the force lines. EHT patches demonstrated a more homogeneous cell distribution than strip-format EHTs[9] and consisted of densely packed elongated cardiomyocytes with advanced sarcomeric structure (Figure 1C and

1D, Movie III in the Data Supplement). Cells mainly expressed the ventricular isoform of myosin light chain (67±1% versus 33±1% myosin light chain, atrial isoform positivity; Figure 1D), demonstrated a more regular sarcomere organization and a lower circularity index than cells that were cultured in 2 dimensions (Figure 1E and 1F). After 3 weeks in culture, 82±4% of the nuclei stained positive for pericentriolar material 1 (PCM1) and only a small number of cells expressed nonmyocyte markers (Figure I in the Data Supplement). Beating frequency after the onset of synchronous beating was 72±7 min^{-1} (n=24) and did not change over time.

Optimization of Culture Conditions

We aimed to establish conditions for stem cell culture, cardiomyocyte differentiation, and EHT generation that contain only reagents available at GMP grade. We therefore (1) replaced Geltrex with vitronectin during stem cell culture and (2) omitted Matrigel during EHT generation. hiPSCs from 3 different lines (including the GMP line TC-1133; Figure II in the Data Supplement) were cultivated under these conditions. Omission of Matrigel did not affect EHT patch development (Figure III in the Data Supplement). Attempts to implement a serum-free protocol[22] resulted in EHT patches (22 EHT patches from 2 hiPSC lines, C25 and UKEi1-A) with sparse cell density that did not acquire a stable synchronous beating pattern (Figure IV in the Data Supplement, Movie IV in the Data Supplement). In contrast, EHT patches cultured in the presence of serum consistently developed a regular synchronous beating pattern (Figure IV in the Data Supplement). Replacement of horse serum with human serum further increased contractility (Figure IV in the Data Supplement, Movie V in the Data Supplement).

Physiological Analysis

Serial contractility measurements were performed in EHT patches from UKEi1-A cardiomyocytes with MUSCLEMOTION[23] after the initiation of synchronous beating. Patch contractility remained stable for 5 days (days 15–20; n=6) before it started to increase until day 25 to 28 (Figure 2A). Absolute force values were determined by (1) calculation from the postdeflection during culture and (2) isometric force measurements in organ bathes. Average EHT patch force was 4.6±0.2 mN in culture and 2.0±0.6 mN in the organ bath. The EHT patches showed higher force when exposed to cumulatively increasing concentrations of isoprenaline (n=11). The sensitivity to isoprenaline (EC_{50}=4 nmol/L) was physiological, and the effect size (+39%) was not different from the effect of direct adenylyl cyclase activation by forskolin or maximally effective external Ca^{2+} concentration (Figure 2B). EHT patches responded with an increase in force with increasing preload (Frank-Starling mechanism; Figure V in the Data Supplement). The force-frequency relationship was evaluated in 3 EHT patches of which 2 demonstrated a positive force-frequency relation up to 2.5 Hz and 1 EHT patch showed no change in force (Figure V in the Data Supplement).

APs were recorded with sharp microelectrodes in EHT patches generated from UKEi1-A. EHT patches beat spontaneously with an average frequency of 1.19±0.10 Hz (n=6). To facilitate comparison with faster beating small-strip EHTs from UKEi1-A (average frequency 1.76±0.15 Hz; n=18), all EHTs were paced at 2 Hz. Human left ventricular tissue was used for comparison. AP shape in EHT patches more closely resembled APs measured in left ventricular tissue than APs from small EHTs (Figure 2C). AP duration (≈280 ms) did not differ between EHT patches and left ventricular tissue over different stimulation rates (Figure 2D) but was significantly shorter in small EHTs. Take-off potential and AP amplitude did not differ between the 3 groups, but maximum upstroke velocity was lower than in left ventricular tissue, both in EHT patches and small EHTs (Figure 2E). Conduction velocity in EHT patches measured at 2 Hz was 41±2 cm/s.

Dose-Finding EHT Patch Transplantation Study

In a pilot study, EHT patches derived from C25, UKEi1-A, or TC-1133 were epicardially transplanted onto cryo-injured guinea pig hearts 7 days after injury. Transplantation of EHT patches with a synchronous beating pattern before transplantation (n=6) resulted in large human grafts, remuscularizing 17±1% (n=6) of the scar area (that amounted to 18±2% of the left ventricular wall; Figure VI in the Data Supplement). Transplantation of EHT patches that did not acquire a stable synchronous beating pattern (under serum-free culture conditions) resulted in small grafts (n=5; Figure VI in the Data Supplement). In a large follow-up dose-finding study, EHT patches were transplanted that contained either no cells (cell-free; n=19), 4.5×10^6 cells (dose 1; n=19), 8.5×10^6 cells (dose 2; n=19), or 12×10^6 cells (dose 3; n=18). EHT patches from dose 1, 2, and 3 developed similarly (average troponin-T expression 85±0.1%; n=56, Figure VII in the Data Supplement). Contractility was assessed with MUSCLEMOTION at the time of transplantation, and the mean did not differ between the 3 groups (Figure VII in the Data Supplement). Hearts were harvested 28 days after transplantation (Figure 3A). Scar area was similar in all groups (23%–29%; Figure 3B and 3C and Figure VIII in the Data Supplement). EHT-patch transplantation resulted in a dose-dependent remuscularization of the scar (dose 1, 1.4±0.4% of the scar area; dose 2, 5.3±2.0%; dose 3, 12.3±2.5%; Figure 3D and Figure VIII in the Data Supplement). Graft size correlated

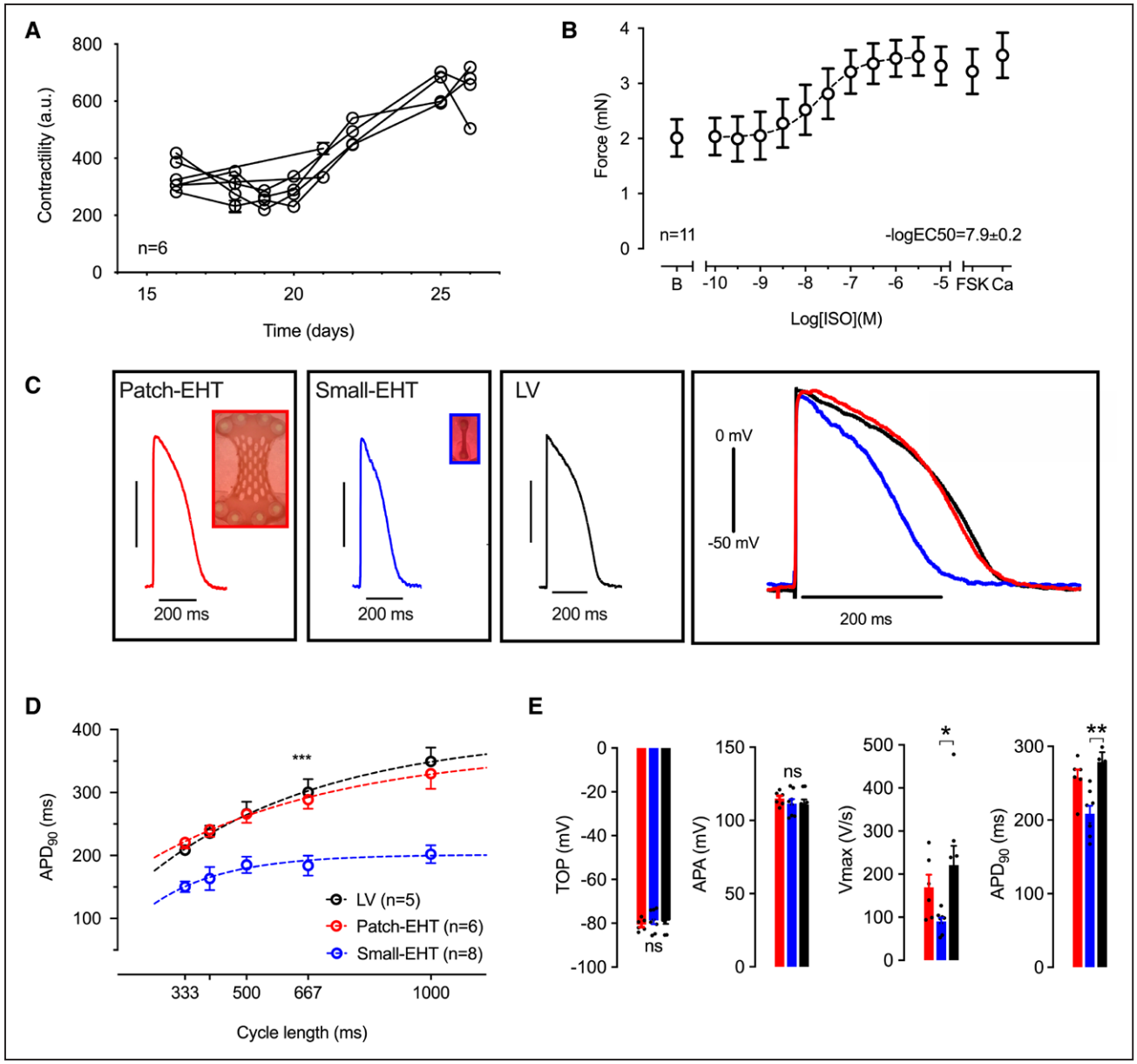

Figure 2. Physiological characterization of human EHT patches.
A, Contractility measurements with MUSCLEMOTION (n=6). First measurement was performed after the initiation of synchronous beating. **B**, Concentration response curve for isoprenaline measured 3 weeks after casting (n=11) in organ bath measurements (Tyrode solution with 1.8 mmol/L calcium). B indicates baseline; Fsk, forskolin (10 µmol/L); and Ca, calcium (8 mmol/L). **C**, Original action potential recordings from EHT patches, small EHTs, and human left ventricular tissue (LV) paced at 2 Hz. **D**, Rate dependency of action potential duration at 90% repolarization (APD_{90}) in EHT patches (red), small EHTs (blue) compared with LV (black). Mean±SEM values are shown. ***P<0.001 for small EHTs compared with LV. **E**, Action potential parameters for EHT patches (red) and small EHTs (blue) compared with LV (black). Multiple action potentials (>5) were measured in each tissue preparation (n=5–8; each data point represents 1 EHT or LV sample). Statistical analyses were performed by 1-way ANOVA followed by Tukey test for multiple comparisons. Mean±SEM values are shown, *P<0.05, **P<0.01. APA indicates action potential amplitude; EHT, engineered heart tissue; and TOP, take-off potential.

with the number of human cells per section (dose 1, 70±140 cells/section; dose 2, 920±280 cells; dose 3, 2250±680 human Ku80$^+$ cells, Figure 3E and Figure VII in the Data Supplement). The estimated grafted cardiomyocyte number was 7.8±2.1×10^6 in dose 3 (cardiomyocyte density 3484±299 cells/mm^2; Figure VII in the Data Supplement). Echocardiography was performed at baseline, before transplantation and 4 weeks after transplantation. EHT patch transplantation improved left ventricular function in the highest dose (fractional area change 46±2% at baseline, 33±2% after injury [–28%], and 41±2% [+8% absolute, +24% relative] 4 weeks after transplantation; Figure 6D), whereas transplantation of EHT patches with lower cell numbers did not improve left ventricular function in comparison with cell-free patches.

Human grafts consisted of densely packed cardiomyocytes with advanced sarcomere structures that almost exclusively expressed MLC2v (97±1% compared with 67±1% in EHT patches before implantation; Figure 4A

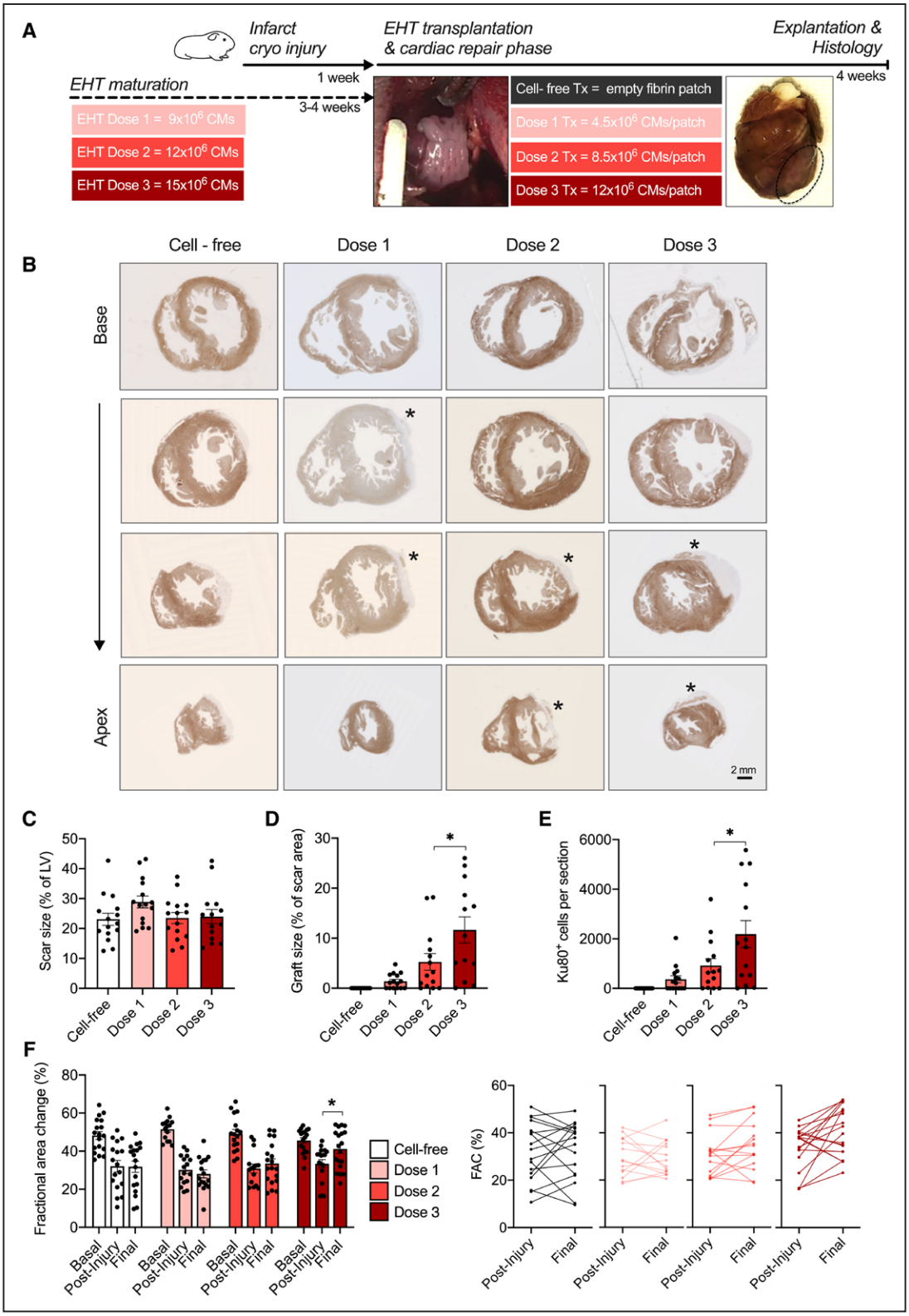

Figure 3. EHT patch transplantation dose-finding study in a guinea pig cryo-injury model.
A, Study design scheme. **B**, Dystrophin-stained short-axis sections from guinea pig hearts of the respective groups. Asterisks mark human grafts. **C**, Scar size quantification as percentage of the left ventricle. Quantification of graft size as percentage of scar area (**D**) and quantification of human Ku80+ cell number per heart section in the respective groups (**E**) 4 weeks after transplantation (n=14–15; each data point represents 1 heart). Statistical analysis was determined by 1-way ANOVA followed by the Tukey test for multiple comparisons **P*<0.05. **F**, Fractional area change values for baseline, postinjury, and 4 weeks after transplantation (n=19 [dose 1/2/cell-free], n=18 [dose 3]). Differences in fractional area change between postinjury and 4 weeks after transplantation. Statistical analysis was determined by 2-way ANOVA followed by the Tukey test for multiple comparisons. **P*<0.05. CMs indicates cardiomyocytes; EHT, engineered heart tissue; FAC, fractional area change; LV, left ventricular tissue; and Tx, transplantation.

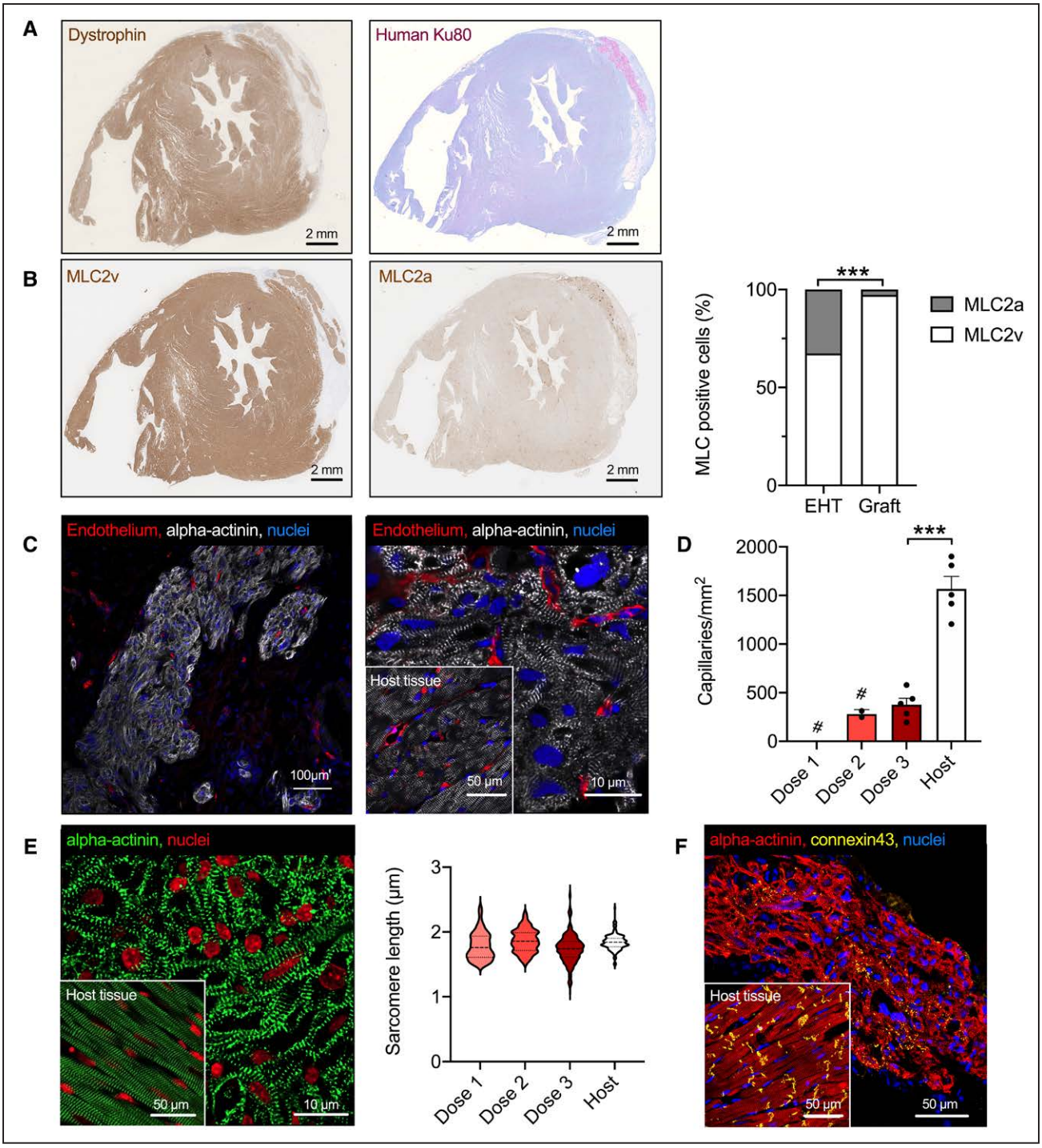

Figure 4. Histological characterization of graft structure.
A, Dystrophin-stained short-axis section from a guinea pig heart of group 3 and human Ku80 staining from an adjacent section. **B**, Myosin light chain, ventricular and myosin light chain, atrial isoform staining of short-axis views, and quantification of myosin light chain isoform expression in the EHT patches before transplantation and in the human grafts 4 weeks after transplantation (n=3 EHT patches or hearts; 2-tailed unpaired Student *t* test, ***P<0.001). **C**, Low and high magnification of a human graft 4 weeks after transplantation stained for α-actinin and endothelium. **D**, Quantification of graft vascularization 4 weeks after transplantation (# indicates that grafts in group 1 were too small for assessment of vascularization and grafts in group 2 were too small for a statistically reliable quantification). n=5 to 10 images/N=3 hearts. Each data point represents 1 heart. Statistical analyses were performed by 2-tailed unpaired Student *t* test, ***P<0.001. **E**, α-Actinin staining and quantification of sarcomere length in human grafts compared with guinea pig host myocardium (n=3 hearts, >50 sarcomeres for graft or host myocardium). Statistical analyses were performed by 1-way ANOVA followed by the Tukey test. **F**, α-Actinin and connexin 43 staining of graft tissue. Insets show host myocardium for comparison. MLC indicates myosin light chain; and EHT, engineered heart tissue.

and 4B) and were vascularized by host-derived vessels (Figure 4C and Figure IX in the Data Supplement). Vascular density within the grafts was lower than in host myocardium (400±60 vessels/mm^2 [dose 3] versus 630±30 vessels/mm^2 in the host myocardium). Quantification for dose 2 was based on a low number of small

grafts, and grafts in dose 1 were too small for quantification (Figure 4D). Human cardiomyocytes were smaller in diameter than cardiomyocytes in host myocardium (diameter 6.0±0.45 µm versus 7.4±0.15 µm; n=75–150 cells/N=3 hearts) and sarcomere length was similar as in host myocardium (Figure 4E). Connexin 43 showed a dispersed expression pattern along the cardiomyocytes, different from the clear intercalated disc pattern in host myocardium (Figure 4F).

Assessment of Cardiomyocyte Proliferation After Transplantation

Three strategies were applied to study cardiomyocyte cell cycle activity after transplantation: double immunolabelling (1) for PCM1 and Ki67 and (2) for human Ku80 and Ki67, and (3) incorporation of bromodeoxyuridine in vivo (Figure 5A–5D). In EHT patches ready for transplantation (21 days after casting), 10±1% of cardiomyocytes were in the cell cycle. Cell cycle activity as determined by Ki67$^+$/PCM1$^+$ double positivity increased after transplantation, reached 20±2% of cardiomyocytes 2 weeks after transplantation and fell to 13±1% after 4 weeks. These results were corroborated by double labeling for human Ku80 and Ki67 that revealed a similar pattern (8±1% Ki67$^+$/Ku80$^+$ nuclei in the EHT patches, 15±4% in the graft after 2 weeks and 10±1% after 4 weeks) and labeling of DNA synthesis by the incorporation of bromodeoxyuridine injected during different periods after transplantation (first week, 13±5%; second week, 21±1%; third week, 7±3%; and fourth week, 14±2%).

Symmetrical expression of Aurora B kinase in rare cases indicated true cardiomyocyte cytokinesis in the grafts (Figure 5E and Figure X in the Data Supplement). To further explore this hypothesis, we assessed graft development over time (Figure 6A and 6B). One week after transplantation, cell density was considerably lower than in the EHT patch at the time of transplantation, and transplanted cardiomyocytes demonstrated little sarcomeric structure (Figure 6B). Two weeks after transplantation, cell density had increased, and cardiomyocyte morphology partially recovered. Scant fibrin matrix was retained 4 weeks after transplantation, and the cardiomyocyte density was substantially higher than in grafts 1 week after transplantation (Figure X in the Data Supplement and Figure 6A and 6B). Cardiomyocyte proliferation is regulated by the Hippo-signaling pathway, which acts via the transcription coactivator YAP (yes-associated protein).[24] Whereas nuclear YAP localization was rare in EHT patches before transplantation, it increased after transplantation (EHT patches, 2±0.4% YAP$^+$ cardiomyocyte nuclei; 1 week after transplantation, 32±7%; 2 weeks after transplantation, 24±2%; and 4 weeks after transplantation, 24±2%; Figure 6C and Figure X in the Data Supplement). In summary, these results indicate that the final graft size depends not purely on cell survival, but also on proliferation.

Upscaling to Human Size

As a next translational step, EHT patches (1.5×2.5 cm) were epicardially transplanted on uninjured pig hearts (2 EHT patches per heart; 2 LEA29 pigs and 3 wildtype animals, weight ≈50 kg). These experiments revealed that the size and stability of the 1.5×2.5 cm EHT patch was not sufficient to withstand the stronger force of the pig heart (compared with guinea pig hearts; Figure XI in the Data Supplement). We hypothesized that upscaling in size, cardiomyocyte density, and fibrin concentration would result in more stable patches. Three human-scale EHT patches were generated as proof-of-principle (5×7 cm, 430–450×10^6 cells; Figure XI in the Data Supplement). The human-scale patches remodeled, and the first macroscopic contractions were visible after 21 days in culture (Figure 7A). Synchronous beating was initiated by electric pacing (2 Hz; Figure 7B and Movie VI in the Data Supplement), and the patches continued to beat synchronously without electric stimulation (Figure 7B and Movie VII in the Data Supplement). Human-scale patches were epicardially transplanted in wildtype (n=2) and LEA29Y pigs (n=2; 1 patch was divided in 2 parts immediately before transplantation). Handling and suturing of human-scale patches on the epicardial surface of uninjured pig hearts was technically easy, and the upscaled patches withstood the mechanical forces during implantation (Figure XI in the Data Supplement). Histological analysis 2 weeks after transplantation revealed small human grafts in the wildtype animals (maximum 650 human cells per section), but larger grafts in the LEA29Y animals (maximum 4500 human cells per section; Figure 7C and Figure XI in the Data Supplement). Screening for immune rejection demonstrated clusters of CD3$^+$ cells in the human grafts (Figure XI in the Data Supplement). Within the surviving human grafts, cell density and cardiomyocyte structure resembled the results seen in guinea pigs 2 weeks after transplantation (Figure 7D).

DISCUSSION

In this study, we aimed to advance the EHT patch approach toward clinical translation by (1) optimizing EHT geometry, (2) establishing a GMP-compatible process for EHT production, (3) determining an effective dose, and (4) exploring the possibility to generate a human-scale patch. In addition, we systematically analyzed cell cycle activity after transplantation.

Optimization of EHT geometry was achieved by integrating and scaling up 2 previously described protocols.[9,21] In contrast to strip-format EHTs, in which cardiomyocytes localize mainly on the outer surface,[9,25] the

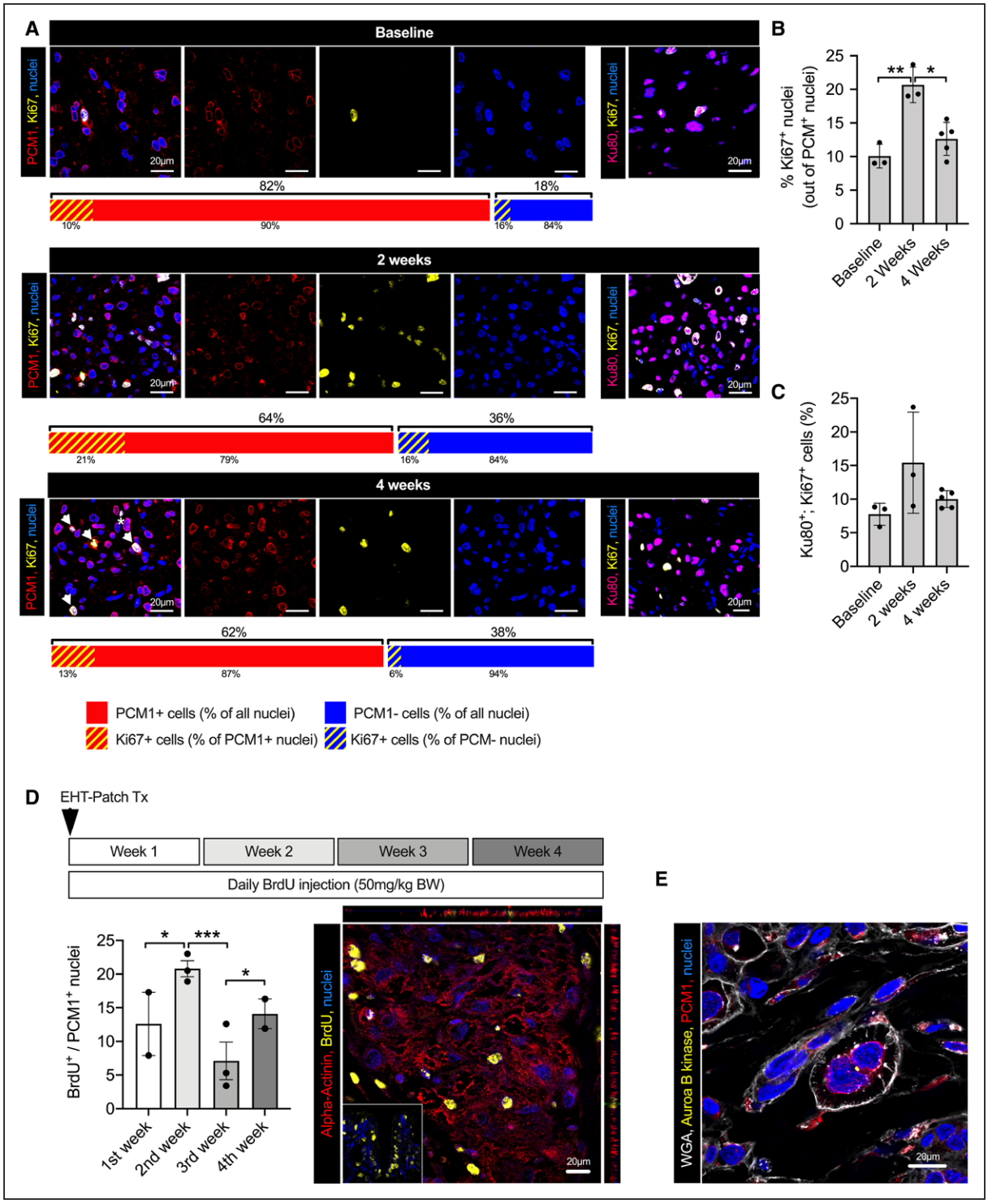

Figure 5. Analysis of cardiomyocyte proliferation and graft development after EHT patch transplantation.
A, PCM1/Ki67 and human Ku80/Ki67 double immunostaining of EHT patches and human grafts 2 and 4 weeks after transplantation. Bar graphs depict the percentage of PCM1-positive and -negative nuclei (% of all nuclei in the EHT or graft) and the Ki67-positive cardiomyocyte and nonmyocyte nuclei at the respective time points. Arrows in lower panel show examples of Ki67-positive/PCM1-positive cells, assumed to be actively cycling cardiomyocytes. The star indicates a Ki67-positive/PCM1-negative nucleus, assumed to be a nonmyocyte in cell cycle. Quantification of Ki67-positive/PCM1-positive nuclei (**B**) and Ki67/Ku80-positive nuclei (**C**; EHT patches: n=600 nuclei/N=3 EHT patches; 2 weeks after transplantation: n=1500 nuclei/N=3 hearts; 4 weeks after transplantation: n=3200 nuclei/N=5 hearts). **D**, Human graft stained for BrdU and α-actinin. BrdU was injected daily over different time periods after transplantation (inset shows small intestine as positive control) and quantification of BrdU-positive cardiomyocytes (300–700 cardiomyocytes/N=2–3 hearts). **E**, Membrane (WGA), PCM1, and Aurora B kinase immunolabeling of a human graft 2 weeks after transplantation. **A** through **E**, Statistical analyses were performed by 1-way ANOVA followed by the Tukey test for multiple comparisons. Mean±SEM values are shown, **P*<0.05, ***P*<0.01. BrdU indicates bromodeoxyuridine; BW, body weight; EHT, engineered heart tissue; PCM1, pericentriolar material 1; and WGA, wheat germ agglutinin.

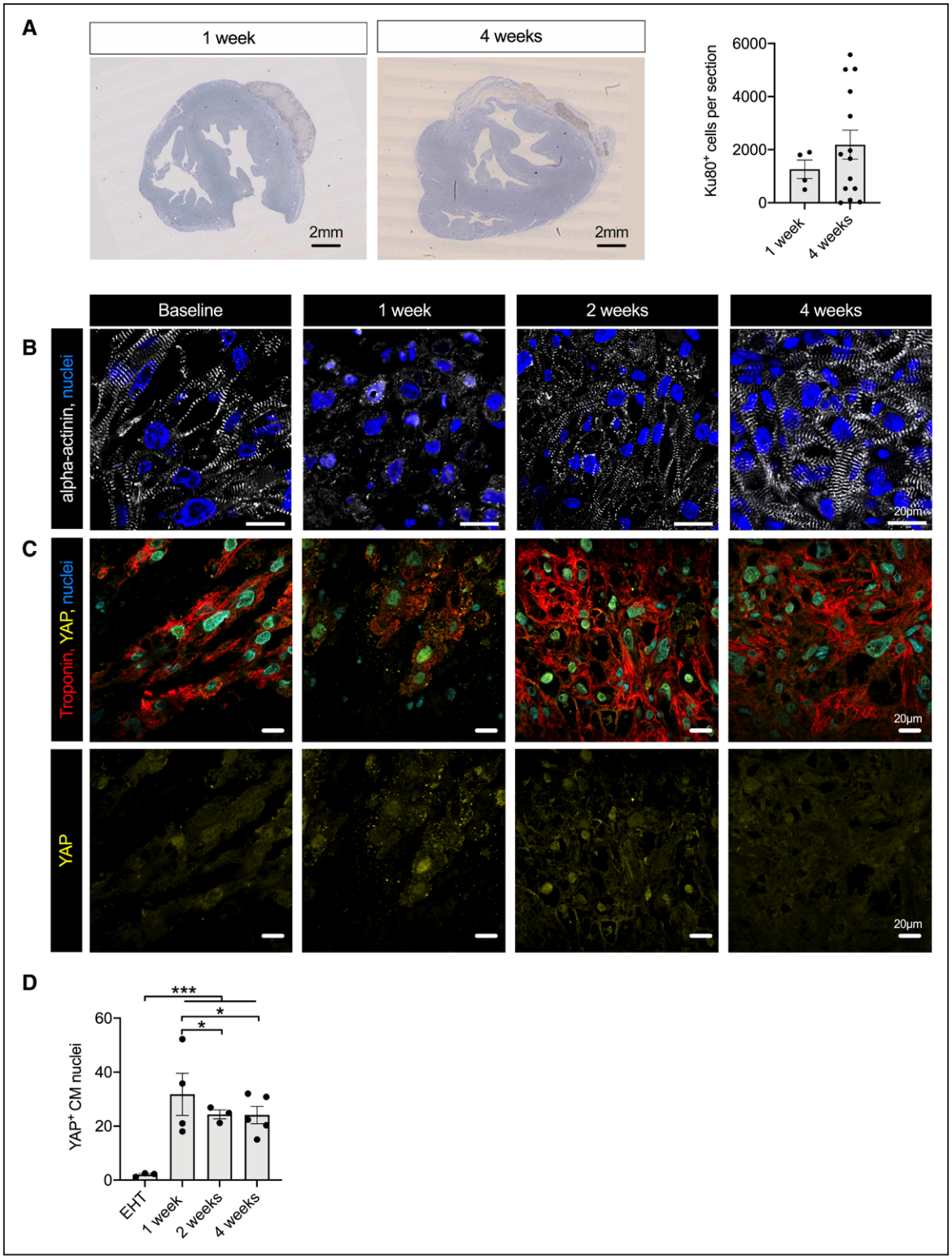

Figure 6. Analysis of graft development after transplantation.
A, Human Ku80 staining of guinea pig heart sections 1 and 4 weeks after transplantation and quantification of human Ku80-positive cells at the respective time points (n= 4 hearts 1 week after transplantation and n=14 hearts 4 weeks after transplantation). Statistical analysis was performed by 2-tailed unpaired Student *t* test. Mean±SEM values are shown. **B**, α-Actinin staining of EHT (baseline) and human grafts 1 week, 2 weeks, and 4 weeks after transplantation. YAP staining (**C**) and quantification (**D**) of nuclear YAP in EHT patches (baseline) and human grafts 1, 2, and 4 weeks after transplantation (n=300 nuclei/N=3–5 EHT patches or hearts, each data point shows 1 EHT patch or heart). Statistical analyses were performed by 1-way ANOVA followed by Tukey test for multiple comparisons. Mean±SEM values are shown, **P*<0.05, ****P*<0.001. CM indicates cardiomyocyte; EHT, engineered heart tissue; and YAP, yes-associated protein.

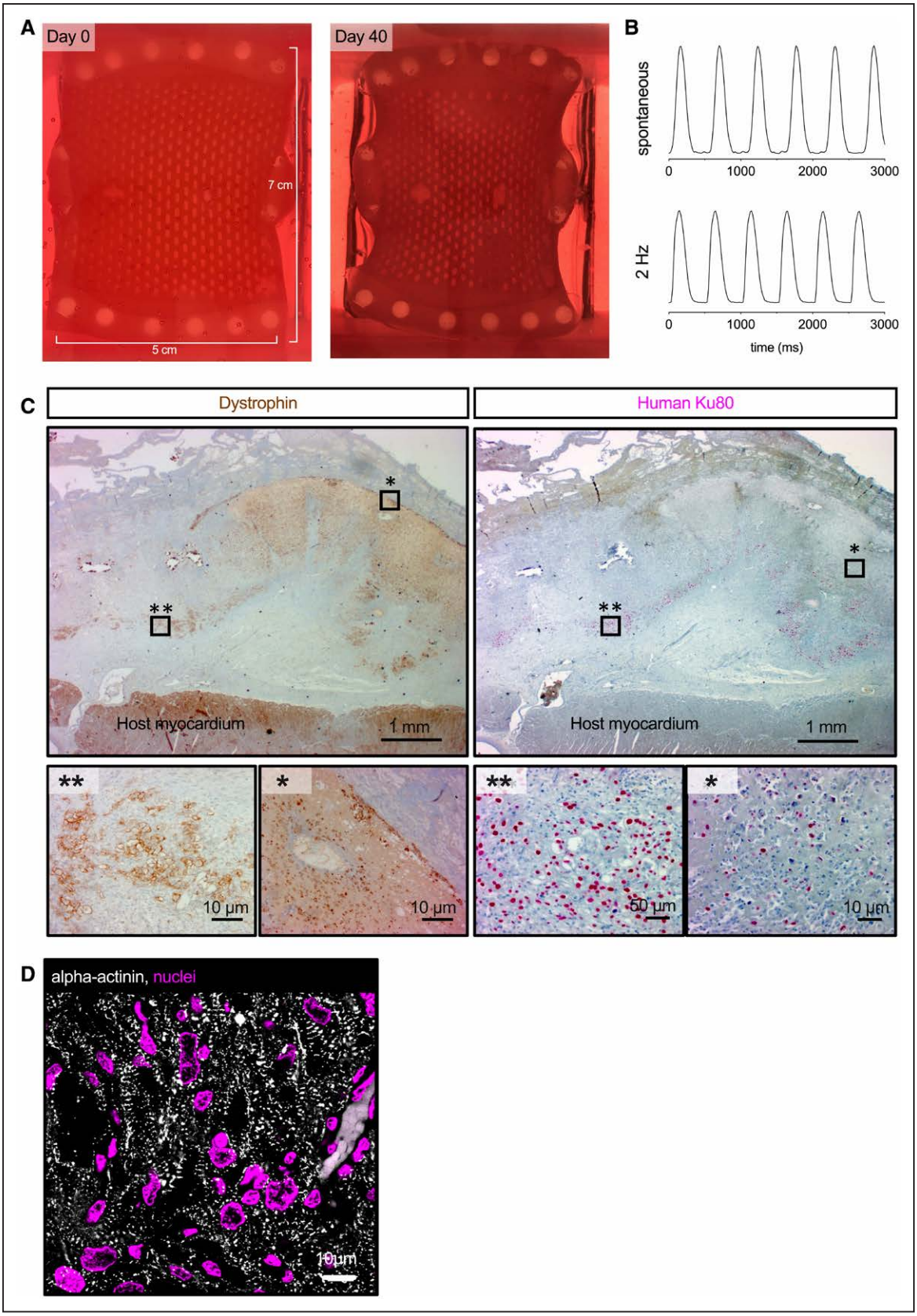

Figure 7. Generation and transplantation of human-scale patches.
A, Photographs of the human-scale engineered heart tissue patch at the time of casting and after 6 weeks in culture. **B**, Contractility measurement of the human-scale engineered heart tissue patch during pacing with 2 Hz and under spontaneous beating. **C**, Anterior wall sections stained for dystrophin and human Ku80 2 weeks after transplantation. Asterisks mark the regions shown in higher magnification. **D**, α-Actinin staining of a human graft 2 weeks after transplantation.

optimized geometry resulted in a dense, homogeneous cardiomyocyte distribution. This can, at least to some extent, be explained by a better nutrition and oxygen supply because we have previously shown that oxygen concentration was low in the center of large tissue patches without mesh structure.[26] Cell distribution was even more homogeneous when we applied dynamic culture conditions,[27] resulting in cardiac patches morphologically resembling mature myocardium. The mature histological phenotype was mirrored by the electrophysiological results. AP characteristics of EHT patches more closely resembled human left ventricular tissue than small EHTs, and the conduction velocity (41 cm/s) was only slightly slower than reported for guinea pig[28] and human myocardium.[29] Despite the morphological and physiological similarity to mature human myocardium, EHT patches also demonstrated signs of immaturity, for example, the expression of MLC2a in some cells[30] and the dispersed expression of connexin 43.[31] Force production per input cardiomyocyte (≈0.3 mN/million cardiomyocytes) was lower than reported recently for similar cardiac constructs,[32] but well in line with standard small EHTs. The fact that the protocol achieved similar results in 3 different iPSC lines (including the GMP-grade hiPSC cell line TC-1133) indicates robustness and general applicability.

Conversion of our standard culture conditions to GMP-like conditions was principally straightforward with one exception. Whereas the omission of Matrigel had no morphological or functional impact, serum turned out to be critical. Serum-free culture of EHTs (according to reference[22]) resulted in macroscopically noncontracting EHT patches and small grafts. Human serum, which is available in GMP grade, gave rise to EHT patches with excellent structure and function. The final protocols thus contained solely substances that are available at GMP grade allowing a potential clinical application.

Although the more mature phenotype of EHTs underlines the effect of optimized culture conditions, it could have resulted in poorer cardiac repair because the transplantation of adult (mature) rat cardiomyocytes was unsuccessful.[33] However, our results indicate that cardiomyocyte maturation (at least to some extent) might even have a favorable effect, for example, when comparing graft results with EHTs cultured under serum-free and serum-containing medium. Graft size per input cell number was similar to strip-format EHT transplantation, but variability was lower[9] and did not differ between EHT patches from different cell lines (UKEi1-A, C25, and TC-1133) that demonstrated a similar, coherent beating pattern (in a small pilot study), indicating that the contractility pattern at the time of transplantation reflects EHT quality (eg, cardiomyocyte maturation, cell-cell interaction) and predicts transplantation success. The grafts consisted of densely packed cardiomyocytes and showed signs of further maturation after transplantation (eg, increased expression of the ventricular isoform and lower expression of the atrial isoform of myosin light chain), but signs of immaturity remained (eg, the dispersed connexin 43 expression and ongoing cell cycle activity). They were vascularized by host-derived vessels within 4 weeks after transplantation, a finding that confirms previous results.[9,34] In contrast to our previous study,[9] and to other recent studies,[22,35,36] we did not include nonmyocytes in the EHT patches. The reason for this was 2-fold. (1) The choice of a single cell type facilitates clinical translation.[37] (2) Nonmyocytes do not directly participate in the formation of new myocytes, the primary goal of remuscularization. Introduction of nonmyocytes mainly aimed to improve patch development and eventually cardiomyocyte engraftment. Yet, we have seen neither positive effects of nonmyocytes on EHT development, nor survival of endothelial cells after transplantation.[9]

The concept of remuscularization is based on the hypothesis that the newly formed myocardium actively contributes to left ventricular function. Even though there is some evidence that improvement in left ventricular function correlates with graft size,[38,39] preclinical studies have not revealed a clear dose dependency.[40] Defining an effective dose therefore represents an important step toward clinical application. Our study demonstrated a cell dose-dependent effect on remuscularization, but the left ventricular function only improved in the highest dose. In fact, a mean graft size of 5% in group 2 was not associated with improved left ventricular function. The estimated number of grafted cells in the high-dose group (12×10^6 cardiomyocytes input) was ≈7.8×10^6 cardiomyocytes amounting to a mass of ≈40 mg grafted cells in a 2.4-g guinea pig heart (graft mass=left ventricular mass [heart mass×0.6] × scar size [% of left ventricle] × graft size [% of scar size]). This reflects a grafted cell mass of ≈16.5 mg/g heart weight. Based on the infarct size of ≈20% of the left ventricle (60% of the total heart mass), one can calculate an engrafted cell mass of ≈140 mg/g infarcted heart mass (infarcted heart mass 0.12 g/g heart weight). These numbers are similar to recently published data in non-human primates (≈100×10^6 engrafted cells in a ≈40-g heart; even though functional improvement was larger in the non-human primate model),[41] indicating that this dosing principle could also be generalized to other animal models or even patients. Assuming a linear relationship ≈1000×10^6 engrafted cardiomyocytes (input EHT-patch cell number ≈1400×10^6 cardiomyocytes; ≈1/3 of the cardiomyocyte number of an adult human heart) would be required for a 300-g heart. Maturation after transplantation and a better functional integration of human cells in a human heart might allow us to apply lower cell numbers, but the number highlights the high ambitions of a cell transplantation strategy.

There is growing evidence that cardiomyocyte proliferation participates in graft development after transplantation of pluripotent stem cell–derived cardiomyocytes.[39,41,42] Yet, a comprehensive analysis was still lacking. We therefore systematically analyzed cardiomyocyte cell cycle activity. A high number of transplanted cardiomyocytes was in the cell cycle with cell cycle activity peaking 2 weeks after transplantation. Analysis of cardiomyocyte proliferation is challenging because (1) it is difficult to distinguish cardiomyocyte from nonmyocyte nuclei and (2) classical markers are not able to discriminate between true proliferation (cytokinesis), polyploidization, and multinucleation. We therefore combined several strategies. They collectively demonstrated an increase in cardiomyocyte cell cycle activity after transplantation. Evidence for true cardiomyocyte proliferation is strengthened by symmetrical midbody localization and the development of graft structure and cardiomyocyte density after transplantation. Early after transplantation, cardiomyocytes had lost the mature phenotype seen in the EHT patch. Cell density in these early grafts was low and sarcomeric structure was irregular, indicating that a substantial number of cardiomyocytes die after transplantation. However, only 1 week later, cell density had increased, and cell morphology improved substantially, most likely reflecting (1) the recovery and maturation of surviving cardiomyocytes and (2) cardiomyocyte proliferation. These results are further corroborated by the analysis of YAP localization. Hippo signaling has been identified as the major pathway to regulate cardiomyocyte proliferation.[24] YAP is a downstream effector of Hippo signaling. In accordance with the expression of cell cycle markers, nuclear YAP expression increased after transplantation. The factors underlying the reentry in the cell cycle are presently unknown, but we hypothesize that hypoxia and increased extracellular stiffness are involved.[43,44] The findings support the strategy to stimulate cardiomyocyte proliferation, either by genetic modifications,[45,46] by pharmacological immunosuppression,[46] or by the addition of other cell types[38] to promote cardiomyocyte transplantation.

When transplanting EHT patches in large animals (≈50 kg), we found that medium-sized patches (1.5×2.5 cm) with a cell density of 15×10^6 cardiomyocytes per 1.5 mL were not suitable for transplantation onto a pig heart. The patches did not withstand the much stronger force of the pig heart. We therefore increased the fibrin concentration and cell density and generated more stable upscaled patches (7×5 cm) containing ≈450 Mio cells. Human-scale patches resisted the mechanical forces of the pig heart, and patch transplantation was technically easy, demonstrating the surgical feasibility of this approach. Given that the human heart contains ≈3×10^9 cardiomyocytes and the surface of the left ventricle is ≈100 cm^2, these EHT patches (35 cm^2) can be safely termed human scale. Yet, the results from our dose-finding study indicate that even higher cell numbers (than the ≈450 Mio currently used) will be required to repair large myocardial injuries in humans. Standard pharmacological immunosuppression resulted in only low cell survival in this xenogeneic setting. Even though more human cells survived short term in transgenic animals overexpressing a human CTLA4-Ig derivate, there was also evidence for T-cell infiltration, demonstrating that inhibition of T-cell costimulation is crucial for the survival of human cardiomyocytes in a pig model,[42] but also highlighting the need for further optimization of immunosuppressive therapy in future large-animal studies.

Limitations

We have chosen a guinea pig model because it resembles the human heart´s electrophysiology better than any other small-animal model. However, the extensive collateralization of the guinea pig heart does not allow the induction of myocardial injuries of reproducible size with an ischemia-reperfusion model.[47,48] We therefore had to use a cryo-injury model. We also did not evaluate heart rhythm in this study because (1) we did not observe arrhythmias in a previous study with EHT strips[49] and (2) small-animal models are of limited validity in arrhythmia prediction. Because human grafts were separated by fibrotic caps from the host tissue, a more detailed analysis of electric coupling will be required in future studies. The large-animal study was designed to show technical feasibility and not efficacy.

Taken together, the present study developed EHT patches with new geometry that exhibit excellent heart tissue structure and function in vitro, can be produced under GMP-compatible conditions, and are mechanically robust and scalable to a human-relevant size. The dose-dependent effect of EHT patch transplantation in a guinea pig model should provide guidance for a relevant cell dose/patch size for a future clinical application.

ARTICLE INFORMATION

Received April 28, 2020; accepted February 16, 2021.

The Data Supplement is available with this article at https://www.ahajournals.org/doi/suppl/10.1161/CIRCULATIONAHA.120.047904.

This manuscript was sent to Prof. Mauro Giacca, Guest Editor, for review by expert referees, editorial decision, and final disposition.

Authors

Eva Querdel; Marina Reinsch, PhD; Liesa Castro, MD; Deniz Köse, MD; Andrea Bähr, DVM; Svenja Reich, BS; Birgit Geertz; Bärbel Ulmer, PhD; Mirja Schulze, PhD; Marc D. Lemoine, MD; Tobias Krause, MD; Marta Lemme, PhD; Jascha Sani; Aya Shibamiya, PhD; Tim Stüdemann, MSc; Maria Köhne, MD; Constantin von Bibra, DVM; Nadja Hornaschewitz, DVM; Simon Pecha, MD; Yusuf Nejahsie, MD; Ingra Mannhardt, PhD; Torsten Christ, MD; Hermann Reichenspurner, MD, PhD; Arne Hansen, MD; Nikolai Klymiuk, PhD; M. Krane, MD; C. Kupatt, MD; Thomas Eschenhagen, MD; Florian Weinberger, MD

Correspondence

Thomas Eschenhagen, MD, Department of Experimental Pharmacology and Toxicology, University Medical Center Hamburg-Eppendorf, Martinistr 52, 20246 Hamburg, Germany; or Florian Weinberger, MD, Department of Experimental Pharmacology and Toxicology, University Medical Center Hamburg-Eppendorf, Martinistr 52, 20246 Hamburg, Germany. Email t.eschenhagen@uke.de or f.weinberger@uke.de

Affiliations

Department of Experimental Pharmacology and Toxicology (E.Q., M.R., D.K., S.R., B.G., B.U., M.S., T.K., M.L., J.S., A.S., T.S., C.v.B., Y.N., I.M., T.C., A.H., T.E., F.W.), Department of Cardiovascular Surgery, University Heart Center (L.C., S.P., H.R.), University Medical Center, Hamburg-Eppendorf, Germany. German Centre for Cardiovascular Research (DZHK), partner site Hamburg/Kiel/Lübeck (E.Q., M.R., L.C., D.K., B.U., M.S., M.D.L., T.K., M.L., J.S., A.S., T.S., M. Köhne, C.v.B., S.P., I.M., T.C., H.R., A.H., T.E., F.W.). I. Medizinische Klinik & Poliklinik, University Clinic Rechts der Isar (A.B., N.H., N.K., C.K.), Department of Cardiovascular Surgery, German Heart Centre Munich (M. Krane), Technical University Munich, Germany. DZHK (German Centre for Cardiovascular Research), partner site Munich Heart Alliance Munich (A.B., N.H., N.K., C.K.). Center for Innovative Medical Models, LMU Munich, Oberschleissheim, Germany (A.B., N.K.). Department of Cardiology-Electrophysiology (M.D.L.), Department of Pediatric Cardiac Surgery (M. Köhne), University Heart Center, Hamburg, Germany. INSURE (Institute for Translational Cardiac Surgery), Cardiovascular Surgery, Munich, Germany (M. Krane). Now with Department of Cardiology and Intensive Care Medicine, University Hospital Schleswig-Holstein, Campus Lübeck, Germany (L.C.).

Acknowledgments

The authors thank K. Hartmann (University Medical Center Hamburg-Eppendorf [UKE], Mouse Pathology Core Facility) for technical assistance in immunohistochemistry and A. Steenpass in contractility studies. They acknowledge J. Starbatty, T. Schulze, B. Klampe, E. Schulze, and J. Eisenmann for technical assistance. They appreciate the contribution of S. Laufer during reprogramming the UKEi1-A line and they thank A. Moretti and K.-L. Laugwitz (University of Munich, Germany) for provision of the C25-hiPSC clone and the National Institute of Neurological Disorders and Stroke Human Cell and Data Repository for providing the TC-1133 cell line. Flow cytometry was conducted in the FACS Core Facility, UKE. The authors particularly thank the laboratory animal facility staff, UKE for their support during the dose-finding study. Author contributions: E. Querdel performed experiments and analyzed data. Dr Reinsch performed experiments, analyzed data, and prepared the manuscript. Dr Castro performed experiments, conducted animal studies, and analyzed data. Dr Köse, S. Reich, and Drs Ulmer and Schulze performed experiments. B. Geertz and Drs Pecha and v. Bibra conducted animal studies and performed experiments. Drs Lemoine, Krause, and Lemme, J. Sani, and Dr Christ performed physiological experiments and analyzed data. Drs Shibamiya, Stüdemann, Köhne, Nejahsie, and Mannhardt performed experiments (human-scale EHT development). Dr Hansen designed experiments and acquired funding. Drs Bähr, Hornaschewitz, Krane, and Kupatt performed transplantation studies in pigs. N.K. developed and provided LEA29Y pigs. Dr Reichenspurner provided technical support and conceptual advice. Drs Eschenhagen and Weinberger designed the project, supervised and performed experiments, acquired funding, and prepared the manuscript.

Sources of Funding

This work was supported by a Late Translational Research Grant from the German Center for Cardiovascular Research (DZHK), (81X2710153 to Drs Eschenhagen and Hansen). E. Querdel was supported by the Werner Otto Stiftung. Dr Köse was supported by a scholarship from the German Society for Cardiology. This study was also supported by the European Research Council (ERC-AG IndivuHeart to Dr Eschenhagen) and the DFG (WE5620/3-1 to Dr Weinberger).

Disclosures

Drs Mannhardt, Hansen, and Eschenhagen are cofounders of EHT Technologies GmbH. A patent describing the generation of human-scale engineered heart tissue patches has been filed. The other authors report no conflicts.

Supplemental Materials

Data Supplement Methods
Data Supplement Tables I–III
Data Supplement Figures I–XI
Data Supplement Movies I–VII

REFERENCES

1. Writing Group Members, Mozaffarian D, Benjamin EJ, Go AS, Arnett DK, Blaha MJ, Cushman M, Das SR, de Ferranti S, Després J-P, et al. Executive summary: heart disease and stroke statistics--2016 update: a report from the American Heart Association. *Circulation* 2016;133:447–454. doi: 10.1161/CIR.0000000000000366
2. Puymirat E, Simon T, Cayla G, Cottin Y, Elbaz M, Coste P, Lemesle G, Motreff P, Popovic B, Khalife K, et al; USIK, USIC 2000, and FAST-MI investigators. Acute myocardial infarction: changes in patient characteristics, management, and 6-month outcomes over a period of 20 years in the FAST-MI Program (French Registry of Acute ST-Elevation or Non-ST-Elevation Myocardial Infarction) 1995 to 2015. *Circulation.* 2017;136:1908–1919. doi: 10.1161/CIRCULATIONAHA.117.030798
3. Townsend N, Wilson L, Bhatnagar P, Wickramasinghe K, Rayner M, Nichols M. Cardiovascular disease in Europe: epidemiological update 2016. *Eur Heart J.* 2016;37:3232–3245. doi: 10.1093/eurheartj/ehw334
4. Eschenhagen T, Bolli R, Braun T, Field LJ, Fleischmann BK, Frisén J, Giacca M, Hare JM, Houser S, Lee RT, et al. Cardiomyocyte regeneration: a consensus statement. *Circulation.* 2017;136:680–686. doi: 10.1161/CIRCULATIONAHA.117.029343
5. Hashimoto H, Olson EN, Bassel-Duby R. Therapeutic approaches for cardiac regeneration and repair. *Nat Rev Cardiol.* 2018;15:585–600. doi: 10.1038/s41569-018-0036-6
6. Gerbin KA, Murry CE. The winding road to regenerating the human heart. *Cardiovasc Pathol.* 2015;24:133–140. doi: 10.1016/j.carpath.2015.02.004
7. Menasché P. Cell therapy trials for heart regeneration - lessons learned and future directions. *Nat Rev Cardiol.* 2018;15:659–671. doi: 10.1038/s41569-018-0013-0
8. Riegler J, Tiburcy M, Ebert A, Tzatzalos E, Raaz U, Abilez OJ, Shen Q, Kooreman NG, Neofytou E, Chen VC, et al. Human engineered heart muscles engraft and survive long term in a rodent myocardial infarction model. *Circ Res.* 2015;117:720–730. doi: 10.1161/CIRCRESAHA.115.306985
9. Weinberger F, Breckwoldt K, Pecha S, Kelly A, Geertz B, Starbatty J, Yorgan T, Cheng KH, Lessmann K, Stolen T, et al. Cardiac repair in guinea pigs with human engineered heart tissue from induced pluripotent stem cells. *Sci Transl Med.* 2016;8:363ra148. doi: 10.1126/scitranslmed.aaf8781
10. Shiba Y, Gomibuchi T, Seto T, Wada Y, Ichimura H, Tanaka Y, Ogasawara T, Okada K, Shiba N, Sakamoto K, et al. Allogeneic transplantation of iPS cell-derived cardiomyocytes regenerates primate hearts. *Nature.* 2016;538:388–391. doi: 10.1038/nature19815
11. Chong JJ, Yang X, Don CW, Minami E, Liu YW, Weyers JJ, Mahoney WM, Van Biber B, Cook SM, Palpant NJ, et al. Human embryonic-stem-cell-derived cardiomyocytes regenerate non-human primate hearts. *Nature.* 2014;510:273–277. doi: 10.1038/nature13233
12. Moretti A, Bellin M, Welling A, Jung CB, Lam JT, Bott-Flügel L, Dorn T, Goedel A, Höhnke C, Hofmann F, et al. Patient-specific induced pluripotent stem-cell models for long-QT syndrome. *N Engl J Med.* 2010;363:1397–1409. doi: 10.1056/NEJMoa0908679
13. Baghbaderani BA, Tian X, Neo BH, Burkall A, Dimezzo T, Sierra G, Zeng X, Warren K, Kovarcik DP, Fellner T, et al. cGMP-manufactured human induced pluripotent stem cells are available for pre-clinical and clinical applications. *Stem Cell Reports.* 2015;5:647–659. doi: 10.1016/j.stemcr.2015.08.015
14. Breckwoldt K, Letuffe-Brenière D, Mannhardt I, Schulze T, Ulmer B, Werner T, Benzin A, Klampe B, Reinsch MC, Laufer S, et al. Differentiation of cardiomyocytes and generation of human engineered heart tissue. *Nat Protoc.* 2017;12:1177–1197. doi: 10.1038/nprot.2017.033
15. Lemoine MD, Mannhardt I, Breckwoldt K, Prondzynski M, Flenner F, Ulmer B, Hirt MN, Neuber C, Horváth A, Kloth B, et al. Human iPSC-derived cardiomyocytes cultured in 3D engineered heart tissue show physiological upstroke velocity and sodium current density. *Sci Rep.* 2017;7:5464. doi: 10.1038/s41598-017-05600-w
16. Lemoine MD, Krause T, Koivumäki JT, Prondzynski M, Schulze ML, Girdauskas E, Willems S, Hansen A, Eschenhagen T, Christ T. Human induced pluripotent stem cell-derived engineered heart tissue as a sensitive test system for QT prolongation and arrhythmic triggers. *Circ Arrhythm Electrophysiol.* 2018;11:e006035. doi: 10.1161/CIRCEP.117.006035

17. Mannhardt I, Saleem U, Mosqueira D, Loos MF, Ulmer BM, Lemoine MD, Larsson C, Améen C, de Korte T, Vlaming MLH, et al. Comparison of 10 control hPSC lines for drug screening in an engineered heart tissue format. *Stem Cell Reports.* 2020;15:983–998. doi: 10.1016/j.stemcr.2020.09.002
18. Bähr A, Käser T, Kemter E, Gerner W, Kurome M, Baars W, Herbach N, Witter K, Wünsch A, Talker SC, et al. Ubiquitous LEA29Y expression blocks T cell co-stimulation but permits sexual reproduction in genetically modified pigs. *PLoS One.* 2016;11:e0155676. doi: 10.1371/journal.pone.0155676
19. Kupatt C, Hinkel R, Horstkotte J, Deiss M, von Brühl ML, Bilzer M, Boekstegers P. Selective retroinfusion of GSH and cariporide attenuates myocardial ischemia-reperfusion injury in a preclinical pig model. *Cardiovasc Res.* 2004;61:530–537. doi: 10.1016/j.cardiores.2003.11.012
20. Weinberger F, Mannhardt I, Eschenhagen T. Engineering cardiac muscle tissue: a maturating field of research. *Circ Res.* 2017;120:1487–1500. doi: 10.1161/CIRCRESAHA.117.310738
21. Zhang D, Shadrin IY, Lam J, Xian HQ, Snodgrass HR, Bursac N. Tissue-engineered cardiac patch for advanced functional maturation of human ESC-derived cardiomyocytes. *Biomaterials.* 2013;34:5813–5820. doi: 10.1016/j.biomaterials.2013.04.026
22. Tiburcy M, Hudson JE, Balfanz P, Schlick S, Meyer T, Chang Liao ML, Levent E, Raad F, Zeidler S, Wingender E, et al. defined engineered human myocardium with advanced maturation for applications in heart failure modeling and repair. *Circulation.* 2017;135:1832–1847. doi: 10.1161/CIRCULATIONAHA.116.024145
23. Sala L, van Meer BJ, Tertoolen LGJ, Bakkers J, Bellin M, Davis RP, Denning C, Dieben MAE, Eschenhagen T, Giacomelli E, et al. MUSCLEMOTION: a versatile open software tool to quantify cardiomyocyte and cardiac muscle contraction in vitro and in vivo. *Circ Res.* 2018;122:e5–e16. doi: 10.1161/CIRCRESAHA.117.312067
24. Wang J, Liu S, Heallen T, Martin JF. The Hippo pathway in the heart: pivotal roles in development, disease, and regeneration. *Nat Rev Cardiol.* 2018;15:672–684. doi: 10.1038/s41569-018-0063-3
25. Hirt MN, Boeddinghaus J, Mitchell A, Schaaf S, Börnchen C, Müller C, Schulz H, Hubner N, Stenzig J, Stoehr A, et al. Functional improvement and maturation of rat and human engineered heart tissue by chronic electrical stimulation. *J Mol Cell Cardiol.* 2014;74:151–161. doi: 10.1016/j.yjmcc.2014.05.009
26. Vollert I, Seiffert M, Bachmair J, Sander M, Eder A, Conradi L, Vogelsang A, Schulze T, Uebeler J, Holnthoner W, et al. In vitro perfusion of engineered heart tissue through endothelialized channels. *Tissue Eng Part A.* 2014;20:854–863. doi: 10.1089/ten.TEA.2013.0214
27. Jackman CP, Carlson AL, Bursac N. Dynamic culture yields engineered myocardium with near-adult functional output. *Biomaterials.* 2016;111:66–79. doi: 10.1016/j.biomaterials.2016.09.024
28. Hara Y, Tamagawa M, Nakaya H. The effects of ketamine on conduction velocity and maximum rate of rise of action potential upstroke in guinea pig papillary muscles: comparison with quinidine. *Anesth Analg.* 1994;79:687–693. doi: 10.1213/00000539-199410000-00012
29. Taggart P, Sutton PM, Opthof T, Coronel R, Trimlett R, Pugsley W, Kallis P. Inhomogeneous transmural conduction during early ischaemia in patients with coronary artery disease. *J Mol Cell Cardiol.* 2000;32:621–630. doi: 10.1006/jmcc.2000.1105
30. Feaster TK, Cadar AG, Wang L, Williams CH, Chun YW, Hempel JE, Bloodworth N, Merryman WD, Lim CC, Wu JC, et al. Matrigel mattress: a method for the generation of single contracting human-induced pluripotent stem cell-derived cardiomyocytes. *Circ Res.* 2015;117:995–1000. doi: 10.1161/CIRCRESAHA.115.307580
31. Angst BD, Khan LU, Severs NJ, Whitely K, Rothery S, Thompson RP, Magee AI, Gourdie RG. Dissociated spatial patterning of gap junctions and cell adhesion junctions during postnatal differentiation of ventricular myocardium. *Circ Res.* 1997;80:88–94. doi: 10.1161/01.res.80.1.88
32. Shadrin IY, Allen BW, Qian Y, Jackman CP, Carlson AL, Juhas ME, Bursac N. Cardiopatch platform enables maturation and scale-up of human pluripotent stem cell-derived engineered heart tissues. *Nat Commun.* 2017;8:1825. doi: 10.1038/s41467-017-01946-x
33. Reinecke H, Zhang M, Bartosek T, Murry CE. Survival, integration, and differentiation of cardiomyocyte grafts: a study in normal and injured rat hearts. *Circulation.* 1999;100:193–202. doi: 10.1161/01.cir.100.2.193
34. Zhang J, Zhu W, Radisic M, Vunjak-Novakovic G. Can we engineer a human cardiac patch for therapy? *Circ Res.* 2018;123:244–265. doi: 10.1161/CIRCRESAHA.118.311213
35. Gao L, Gregorich ZR, Zhu W, Mattapally S, Oduk Y, Lou X, Kannappan R, Borovjagin AV, Walcott GP, Pollard AE, et al. Large cardiac muscle patches engineered from human induced-pluripotent stem cell-derived cardiac cells improve recovery from myocardial infarction in swine. *Circulation.* 2018;137:1712–1730. doi: 10.1161/CIRCULATIONAHA.117.030785
36. Ye L, Chang YH, Xiong Q, Zhang P, Zhang L, Somasundaram P, Lepley M, Swingen C, Su L, Wendel JS, et al. Cardiac repair in a porcine model of acute myocardial infarction with human induced pluripotent stem cell-derived cardiovascular cells. *Cell Stem Cell.* 2014;15:750–761. doi: 10.1016/j.stem.2014.11.009
37. Stevens KR, Murry CE. Human pluripotent stem cell-derived engineered tissues: clinical considerations. *Cell Stem Cell.* 2018;22:294–297. doi: 10.1016/j.stem.2018.01.015
38. Bargehr J, Ong LP, Colzani M, Davaapil H, Hofsteen P, Bhandari S, Gambardella L, Le Novère N, Iyer D, Sampaziotis F, et al. Epicardial cells derived from human embryonic stem cells augment cardiomyocyte-driven heart regeneration. *Nat Biotechnol.* 2019;37:895–906. doi: 10.1038/s41587-019-0197-9
39. Sun X, Wu J, Qiang B, Romagnuolo R, Gagliardi M, Keller G, Laflamme MA, Li R, Nunes SS. Transplanted microvessels improve pluripotent stem cell–derived cardiomyocyte engraftment and cardiac function after infarction in rats. *Sci Transl Med* 2020;12:eaax2992.
40. Weinberger F, Eschenhagen T. Cardiac regeneration: new hope for an old dream. *Annu Rev Physiol.* 2021;83:59–81. doi: 10.1146/annurev-physiol-031120-103629
41. Liu YW, Chen B, Yang X, Fugate JA, Kalucki FA, Futakuchi-Tsuchida A, Couture L, Vogel KW, Astley CA, Baldessari A, et al. Human embryonic stem cell-derived cardiomyocytes restore function in infarcted hearts of non-human primates. *Nat Biotechnol.* 2018;36:597–605. doi: 10.1038/nbt.4162
42. Romagnuolo R, Masoudpour H, Porta-Sánchez A, Qiang B, Barry J, Laskary A, Qi X, Massé S, Magtibay K, Kawajiri H, et al. Human embryonic stem cell-derived cardiomyocytes regenerate the infarcted pig heart but induce ventricular tachyarrhythmias. *Stem Cell Reports.* 2019;12:967–981. doi: 10.1016/j.stemcr.2019.04.005
43. Kimura W, Nakada Y, Sadek HA. Hypoxia-induced myocardial regeneration. *J Appl Physiol (1985).* 2017;123:1676–1681. doi: 10.1152/japplphysiol.00328.2017
44. Vite A, Zhang C, Yi R, Emms S, Radice GL. α-Catenin-dependent cytoskeletal tension controls Yap activity in the heart. *Development.* 2018;145:dev149823. doi: 10.1242/dev.149823
45. Zhu W, Zhao M, Mattapally S, Chen S, Zhang J. CCND2 overexpression enhances the regenerative potency of human induced pluripotent stem cell-derived cardiomyocytes: remuscularization of injured ventricle. *Circ Res.* 2018;122:88–96. doi: 10.1161/CIRCRESAHA.117.311504
46. Fan C, Fast VG, Tang Y, Zhao M, Turner JF, Krishnamurthy P, Rogers JM, Valarmathi MT, Yang J, Zhu W, et al. Cardiomyocytes from CCND2-overexpressing human induced-pluripotent stem cells repopulate the myocardial scar in mice: a 6-month study. *J Mol Cell Cardiol.* 2019;137:25–33. doi: 10.1016/j.yjmcc.2019.09.011
47. Maxwell MP, Hearse DJ, Yellon DM. Species variation in the coronary collateral circulation during regional myocardial ischaemia: a critical determinant of the rate of evolution and extent of myocardial infarction 1987:737–746. doi: 10.1093/cvr/21.10.737
48. Lindsey ML, Bolli R, Canty JM Jr, Du XJ, Frangogiannis NG, Frantz S, Gourdie RG, Holmes JW, Jones SP, Kloner RA, et al. Guidelines for experimental models of myocardial ischemia and infarction. *Am J Physiol Heart Circ Physiol.* 2018;314:H812–H838. doi: 10.1152/ajpheart.00335.2017
49. Pecha S, Yorgan K, Röhl M, Geertz B, Hansen A, Weinberger F, Sehner S, Ehmke H, Reichenspurner H, Eschenhagen T, et al. Human iPS cell-derived engineered heart tissue does not affect ventricular arrhythmias in a guinea pig cryo-injury model. *Sci Rep.* 2019;9:9831. doi: 10.1038/s41598-019-46409-z